Available online at www.sciencedirect.com
SCIENCE DIRECT®
Bioorganic & Medicinal Chemistry
ELSEVIER
Bioorganic & Medicinal Chemistry 12 (2004) 1689–1695

# Design, synthesis and in vitro antitumor activity of new *trans* 2-[2-(heteroaryl)vinyl]-1,3-dimethylimidazolium iodides

Francesco P. Ballistreri,[a] Vincenza Barresi,[a] Paolo Benedetti,[b] Gianluigi Caltabiano,[a] Cosimo G. Fortuna,[a] Maria L. Longo[a] and Giuseppe Musumarra[a,*]

[a]*Dipartimento Scienze Chimiche, Università di Catania, V.le A.Doria 6, 95125, Catania, Italy*
[b]*Dipartimento Chimica, Università di Perugia, Via Elce di Sotto 8, 06100, Perugia, Italy*

Received 14 October 2003; accepted 13 January 2004

**Abstract**—The design, the synthesis, and the in vitro antitumor activities of *trans* 2-[2-(heteroaryl)vinyl]-1,3-dimethylimidazolium iodides versus MCF7 (human mammary carcinoma) and LNCap (prostate carcinoma) cell lines are reported. The design indicates *trans* 2-[2-[5-(2-chlorophenyl)furan-2-yl]vinyl]-1, 3-dimethylimidazolium iodide **5** and *trans* 2-[2-[5-(4-bromophenyl)furan-2-yl]vinyl]-1, 3-dimethylimidazolium iodide **6** as highly active compounds in the series. The synthesis of the above new derivatives and in vitro antitumor tests, confirm their significant antiproliferative and cytotoxic activities.


## 1. Introduction

New 2,6-di-[2-(heteroaryl)vinyl]pyridines and pyridiniums,[1,2] where three heteroaromatics rings are linked by two ethylenic double bonds exerting a 'spacing' function, as well as *trans* 1-heteroaryl-2-(1-methylpyridinium-2-yl) ethylenes, where two heteroaromatics are linked by a single ethylenic bridge, exhibited in vitro antitumour activity.[3,4] Tests against two tumor cell lines, breast carcinoma (MCF7) and prostate carcinoma (LNCap), indicating 2,6-di-[2-(furan-2-yl)vinyl]pyridinium iodide and 1-[5-(4-Bromophenyl)-furan-2-yl]-2-(1-methyl-pyridinium-2-yl)ethylene as the most active compounds, suggest that the presence of three aromatic rings and of an halogen atom might increase the anti-proliferative activity. Following these leads, we here report on the design of new *trans* 2-[2-(heteroaryl)vinyl]-1,3-dimethylimidazolium iodides **1–10** in order to orient the synthesis and tests on the in vitro antitumor activity of selected derivatives.

Molecular modelling was performed by means of a Molecular Interaction Field (MIF) approach using Grid Independent Descriptors (GRIND)[5] calculated using the program ALMOND [www.moldiscovery.com].

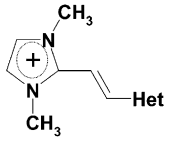


| | Het |
|---|---|
| 1 | Furan-2-yl |
| 2 | 5-Methylfuran-2-yl |
| 3 | 5-Bromofuran-2-yl |
| 4 | 5-Phenyl-furan-2-yl |
| 5 | 5-(2-Chlorophenyl)-furan-2-yl |
| 6 | 5-(4-Bromophenyl)-furan-2-yl |
| 7 | Thiophen-2-yl |
| 8 | 5-Bromo thiophen-2-yl |
| 9 | N-Methylpyrrol-2-yl |
| 10 | Thiazol-2-yl |

**Scheme 1.**

## 2. Results and discussion

In classic 3D-QSAR the alignment (i.e., selection of an appropriate relative orientation of the compounds in

*Keywords:* Antitumor compds; Molecular modelling; Heterocycles; QSAR.
* Corresponding author. Tel.: +39-095-334175; fax: +39-095-580138; e-mail: gmusumarra@dipchi.unict.it

0968-0896/$ - see front matter © 2004 Elsevier Ltd. All rights reserved.
doi:10.1016/j.bmc.2004.01.018

the series) represents a most difficult and time-consuming step. A novel methodology for producing a mathematical description of molecules called GRIND was found to be highly relevant with respect to biological properties and therefore applicable in many different areas of drug design. An important peculiarity of these novel descriptors is that they are insensitive to the position and orientation of the molecular structures in the space. Therefore, since the GRIND needs no alignment of compounds, 3D-QSAR analysis requires less time as compared to standard methodologies. Moreover the use of these descriptors is not limited to 3D-QSAR, and allows to extend their application in 3D searching, pharmacophore identification, and structure-metabolism relations.

The 3D structures of compounds **1**–**10** and for 2,6-di-[2-(furan-2-yl)vinyl]pyridinium iodide **11**, reported for comparisons, were imported, in Mol-file, and coded as ALMOND descriptors following the procedure described in the Computational Methods section.

The process of ligand-receptor interaction can be represented with the help of the MIF. If a compound is known to bind a certain receptor, some of the regions defined in its Virtual Receptor Site (VRS)[5] should actually overlap groups of the real receptor site and, therefore, at least a subset of the VRS regions should be relevant for representing the binding properties of the ligand.

To obtain relevant VRS, it is necessary to adopt probes resembling potentially important groups of the binding site. For compounds interacting with proteins, it seems reasonable to use the DRY probe representing hydrophobic interactions, the O probe (carbonyl oxygen) to represent hydrogen bond acceptor groups, and the N1 probe (amide nitrogen) to represent hydrogen bond donor groups.

Principal Components Analysis (PCA) of ALMOND descriptors relative to compounds **1**–**11** afforded a 5 PC model explaning 81.4% of variance, 34.9% 1st PC, 17.8% 2nd PC, 17.7% 3rd PC, 5.7% 4th PC and 5.3% 5th PC. Figure 1, the scores plot depicting the data structure elucidated by 3 PC (already explaining more than 70% of variance) appears a simplified graphical representation for an immediate evaluation of 3D structural MIF results for compounds **1**–**11** when interacting with the three above mentioned probes.

In Figure 1, 2,6-di-[2-(furan-2-yl)vinyl]pyridinium iodide **11**, the most active compound previously synthesized by our group, exhibits a high value in×axis, which can reasonably be assumed as a direction representative of antitumor activities. According to the above interpretation, compounds **4** and **5** should be more active than other in the series, and *trans* 2-[2-[5-(4-bromophenyl)-furan-2-yl]vinyl]-1, 3-dimethylimidazolium iodide **6** even more active than **11**. This result is consistent with our hypothesis that the presence of three aromatic

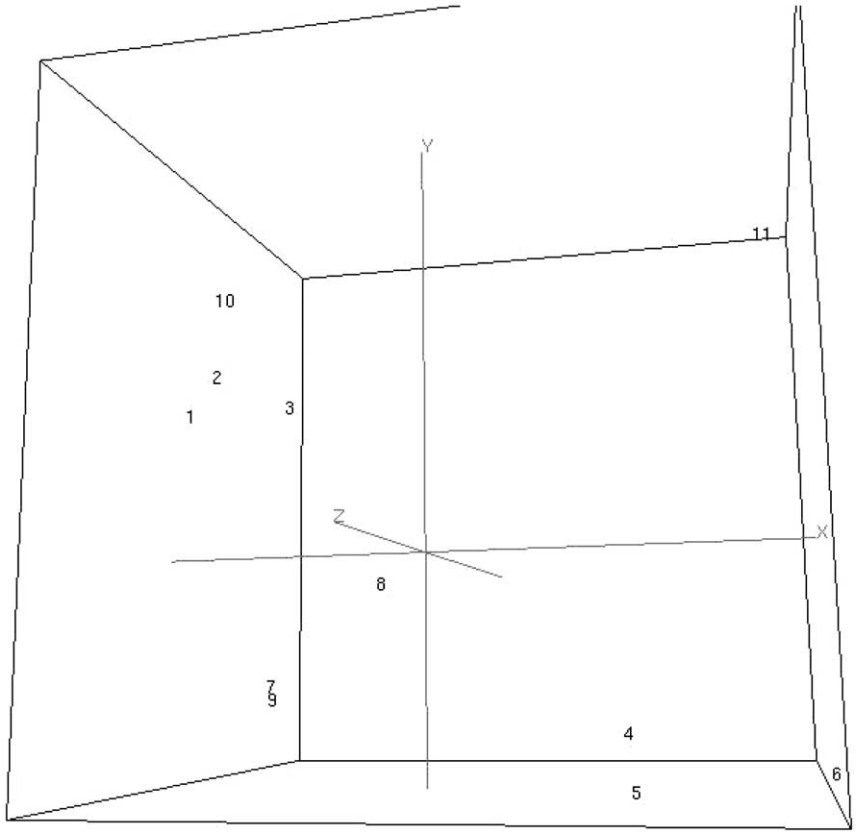


**Figure 1.** Three components PCA scores plot for compounds **1**–**11**.

**Table 1.** In vitro antitumor activities, expressed as log $GI_{50}$, for MCF7 and LNCap cell line

| Cell line/Compounds | 1 | 2 | 3 | 5 | 6 | 8 | 9 | 11 |
|---|---|---|---|---|---|---|---|---|
| MCF7 (breast) | > −4 | −4.48 | −4.40 | −5.86 | −6.21 | −4.84 | > −4 | −6.00 |
| LNCap (prostate) | > −4 | −4.78 | > −4 | −5.38 | −5.42 | −4.52 | > −4 | −5.23 |

moieties and of halogen atoms should increase activity. In order to verify the above hypothesis we proceeded with the synthesis and in vitro biological evaluation of selected derivatives in Scheme 1.

The synthesis of *trans* 2-[2-(heteroaryl)vinyl]-1,3-dimethylimidazolium iodides **1**–**10** can be achieved by condensation of 1,2,3-trimethyl imidazolium iodide with heteroaromatic aldehydes in the presence of NaOH (see Experimental), exploiting the acidity of imidazolium α methyl groups due to the adjacent ring nitrogen positive charge.

Under appropriate experimental conditions pure *trans* isomers **1**–**3**, **5**, **6**, **8**–**10** were obtained, as evidenced by the ethylenic protons J coupling constants in the NMR spectra (see Experimental). Reaction of 2-thiophenaldehyde with 1,2,3-trimethyl imidazolium iodide in the presence of NaOH afforded the *cis* **7** isomer as shown by ethylenic protons J coupling constants in the NMR spectra and by a NOE experiment (see Experimental). Attempts to synthesize the *trans* isomer, as well as 5-phenyl furan derivative **4,** were unsuccessful.

The anti-proliferative activity of compounds **1-3**, **5**, **6**, **8** and **9** was tested against two tumor cell lines, breast carcinoma (MCF7) and prostate carcinoma (LNCap). The in vitro activities, expressed as log $GI_{50}$ values (see Experimental), are recorded in Table 1, together with those of 2,6-di-[2-(furan-2-yl)vinyl]pyridinium iodide **11**, the most active compound in previous in vitro tests,[3] also reported for comparisons. It is worth mentioning that, in order to obtain comparable biological tests, log $GI_{50}$ in Table 1 were all measured in the same experiment. Discrepancies from log $GI_{50}$ values recorded in ref 3 for **11** are not surprising taking into account the variability of biological tests and the higher number of cell passages of the cell line used in the present experiment (30) with respect to those (20) adopted in previous in vitro tests.[4]

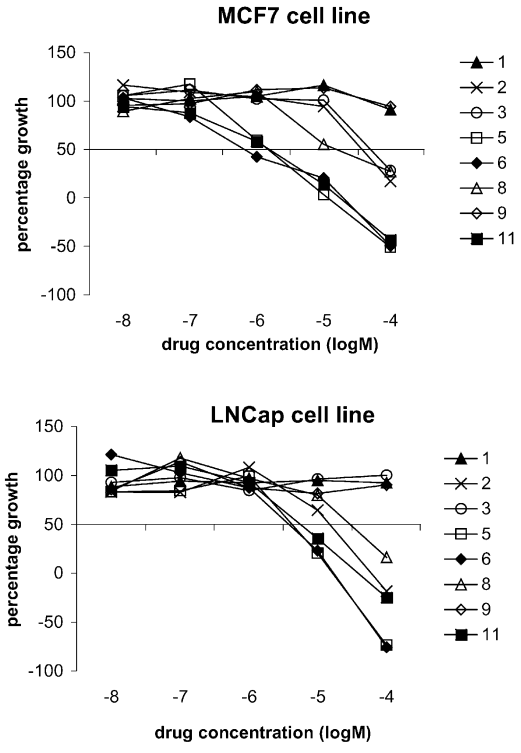


**Figure 2.** Dose–response curves of the antiproliferative activities of compounds **1** (▲), **2** (×), **3** (○), **5** (□), **6** (◆), **8** (△), **9** (◇) and **11** (■) on MCF7 and LNCap cell lines.

According to molecular modelling, *trans* 2-[2-[5-(2-chlorophenyl)furan-2-yl]vinyl]-1,3-dimethylimidazolium iodide **5**, exhibits antiproliferative activity (log $GI_{50}$) similar to that of $PF_2$ **11**, and *trans* 2-[2-[5-(4-bromophenyl)furan-2-yl]vinyl]-1,3-dimethylimidazolium iodide **6**, even higher. Experimental biological data in Table 1 are in close agreement with the model predictions, corroborating the validity of our approach for the design of more active molecules. Growth inhibition of MCF7 is in general higher than that of LNCap cell lines.

The percent of growth and the inhibition exerted by different doses (0.01–100 μM) are recorded in Figure 2. In addition to antiproliferative effects (log $GI_{50}$), the chlorophenyl and bromophenyl derivatives **5** and **6** exhibit a significant cytotoxic activity, expressed as $\log LC_{50}$ values (−4.00 for both compounds versus MCF7 cells and −4.22 and −4.23 respectively versus LNCap cells), especially versus prostate carcinoma cells. This finding points to **5** and **6** as possible lead compounds for future antitumor studies.

## 3. Conclusions

The design of new *trans* 2-[2-(heteroaryl)vinyl]-1,3-dimethylimidazolium iodides, performed by means of a Molecular Interaction Field (MIF) approach using Grid Indipendent Descriptors (GRIND), indicates derivatives **5** and **6** as more active compounds for the growth inihibition of MCF7 and LNCap antitumor cells. The synthesis of the designed ethylenes and experimental in vitro tests parallel the design predictions.

## 4. Experimental

### 4.1. Computational methods

MIF were obtained using the program GRID version 20.[6] GRIND were generated, analysed, and inter-

preted using the program ALMOND version 3.0.0 [www.moldiscovery.com] a software package developed in our group. Computations and graphical display were performed on SGI O2 workstations (MIPS R12000 processor). The process of ligand-receptor interaction has often been represented with the help of the MIF.

If a compound is known to bind a certain receptor, some of the regions defined in its Virtual Receptor Site (VRS)[5] should actually overlap groups of the real receptor site and, therefore, at least a subset of the VRS regions would be relevant for representing the binding properties of the ligand. For the latter statement to be true the VRS must have been obtained from the bioactive conformation of the ligand and the probes used to compute it should represent chemical groups present in the binding site. The molecular descriptors presented in this work are based on the concept of VRS. Basically, GRIND are a small set of variables representing the geometrical relationships between relevant regions of the VRS and as such are independent of the coordinate frame of the space where the MIF is computed. The procedure for obtaining GRIND involves three steps: (i) computing a set of MIF, (ii) filtering the MIF to extract the most relevant regions that define the VRS, and (iii) encoding the VRS into the GRIND variables.

**(i) Computing the MIF.** To obtain relevant VRS, the probes used should represent potentially important groups of the binding site. For compounds interacting with proteins, it seems reasonable to use the DRY probe representing hydrophobic interactions, the O probe (carbonyl oxygen) to represent hydrogen bond acceptor groups, and the N1 probe (amide nitrogen) to represent hydrogen bond donor groups. In default mode a grid-spacing of 0.5 Å is used with the grid extending 5 Å beyond a molecule.

**(ii) Filtering the MIF.** For our purposes, we define the most interesting regions as those characterized by intense favourable (negative) energies of interaction. Unfortunately, a simple contouring procedure would not allow all such regions to be identified, as a region representing a very intense interaction can mask other interactions induced by different parts of the ligand. Instead we have developed a procedure that extracts these 'relevant regions' using an optimisation algorithm, selecting from each MIF a fixed number of nodes optimising a scoring function. This function includes two optimality criteria: the intensity of the field at a node and the mutual node-node distances between the chosen nodes. Therefore, the method extracts from each field a number of nodes (in the order of 150–200) that represent independent, favourable probe-ligand interaction regions. By default, the procedure provides a balanced solution, but sometimes, when the ligands contain charged groups or many polar substituents, the importance of the field values should be decreased, to extract all the recognizable independent regions. Another important parameter of the procedure is the number of extracted nodes. The method uses as a default a value of 150, which is enough in most cases, but for compounds with complex structures this number can be increased.

**(iii) Encoding the VRS into GRIND.** As mentioned above, GRIND encodes the geometrical relationships between the VRS regions in such a way that they are no longer dependent upon their positions in the 3D space. Basically, the encoding is an auto- and cross-correlation transform.[5] The procedure works on the filtered nodes extracted by the previous step and computes the product of the interaction energy for each pair of nodes. The results of the products are handled according to the distance between the nodes. A discrete number of categories, each one representing a small rank of distances, are considered. In regular autocorrelation analysis, all computed terms are summed, and the result characterizes each category. In our approach, only the highest product is stored, while others are discarded. This important difference is responsible for the 'reversibility' properties of GRIND. A sum cannot be reverted to all its terms but the nodes producing the maximum product can be stored in the computer memory and traced back when necessary. Accordingly, this method is called maximum auto- and cross-correlation (MACC) or, more specifically, MACC-2.[5] The values obtained from the analysis can be represented directly in correlogram plots, where the products of the node–node energies are reported versus the distance separating the nodes. One single energy value is obtained for each of the categories considered and represents a small distance range. Molecular description: GRID Force Field. The GRID program[7–9] was used to describe the molecular structures. GRID is a computational procedure for detecting energetically favourable binding sites on molecules. The program calculates the interactions between the molecule and a probe group which is moved through a regular grid of points in a region of interest around the target molecule and, at each point, the interaction energy between the probe and the target molecule is calculated as the sum of Lennard-Jones ($E_{LJ}$), hydrogen bond ($E_{HB}$) electrostatic interactions ($E_{EL}$) and, for specific probes, entropic contribution ($E_{ENT}$):

$$E_{x,y,z} = \sum_{i=1}^{N} E_{LJ} + \sum_{i=1}^{N} E_{HB} + \sum_{i=1}^{N} E_{EL} + \sum_{i=1}^{N} E_{ENT}$$

GRID contains a table of parameters to describe each type of atom occurring in each of the ligand molecules. These parameters define the strength of the Lennard-Jones, hydrogen bond and electrostatic interactions made by an atom and are used in order to evaluate the energy functions. GRID probes are very specific. They give precise spatial information, and this specificity and sensitivity are an advantage since the probes may then be representative of the important chemical groups present in the active site provided that the statistical method used for the analysis can distinguish between different types of interactions.

## 5. Compounds

Heteroaromatic carboxaldehydes were Aldrich commercial products.

UV-Vis spectra were recorded on a Perkin Elmer Lambda 2S spectrometer

$^1$H NMR spectra were recorded on a Varian Unity *Inova* spectrometer operating at 500 MHz, at 25 °C in $(CD3)_2SO$ using TMS or acetone (2.225 ppm) as internal standards. The spectral width was set to 5000 Hz, with an excitation pulse of 60°, an acquisition time of 3.5 s and a digital resolution after zero-filling of 0.15 Hz/pt.

Fast Atom Bombardment (FAB) mass spectra were recorded on a double focusing Kratos MS 50 mass spectrometer equipped with the standard FAB source and the Maspec2 data acquisition and processing system (Mass Spectrometry Services Ltd). Mass resolution was 3,000 and the matrix 3-nitro-benzyl alcohol.

1-Heteroaryl-2-(1,3-dimethylimidazolium-2-yl) ethylenes, all iodide salts, were obtained by refluxing in ethanol equimolar amounts of 1,2,3-trimethylimidazolium iodide and the appropriate heteroaromatic aldehyde in the presence of few drops 20% NaOH. The resulting precipitate was recrystallized from ethanol.

Details on the synthetic conditions and products characterization are reported below:

### 5.1. *trans* 2-[2-(Furan-2-yl)vinyl]-1,3 dimethylimidazolium iodide (1)

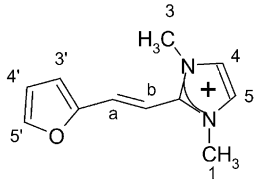


From 2-furan aldehyde (86.21 μL, 1.04 mmol) and 1,2,3 trimethylimidazolium iodide (0.248 g, 1.04 mmol), 2 mL ethanol, 2 drops of NaOH, 5 min. Light pink needles. Yield: 209 mg (63.5%); mp 293–295 °C (lit.[10] no mp or NMR available); MS: *m*/*z* 189; $^1$H NMR(DMSO-$d_6$, δ): 7.45 (d,1H, $J$ = 16.5 Hz, Ha), 6.89 (d,1H, $J$ = 16.5 Hz, Hb), 3.90 (s, 6H,H1,H3), 7.73 (s, 2H, H4,H5), 7.94 (d, 1H, $J$ = 1.5 Hz, H5′), 6.71 (m, 1H, $J$ = 3.5 Hz, H4′), 6.97 (d, 1H, $J$ = 3.5 Hz, H3′). Anal. calcd for $C_{11}H_{14}IN_2O$: C, 69.45; H, 7.42; N, 14.72. Found: C, 69.31; H, 7.39; N, 14.89.

### 5.2. *trans* 2-[2-(5-Methylfuran-2-yl)vinyl]-1,3 dimethylimidazolium iodide (2)

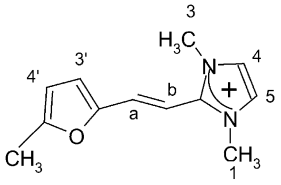


From 5-methylfuran aldehyde (37 mg, 0.334 mmol) and 1,2,3 trimethylimidazolium iodide (80 mg, 0.334 mmol), 2 mL ethanol, 4 drops NaOH. The solution was stirred, 15 min. Yellow prisms. Yield: 36 mg (32%); mp 232–233 °C; MS: *m*/*z* 204; $^1$HNMR (DMSO-$d_6$, δ): 6.42 (d,1H, $J$ = 16.5 Hz, Ha), 5.79 (d, 1H, $J$ = 16.5 Hz, Hb), 2.93 (s, 6H, H1, H3), 6.75 (s, 2H, H4, H5), 2.79 (s, 3H, H5′), 5.40 (d, 1H, $J$ = 3.5 Hz, H4′), 5.91 (d, 1H, $J$ = 3.5 Hz, H3′). Anal. calcd for $C_{12}H_{16}IN_2O$: C, 70.87; H, 9.15; N, 12.72. Found: C, 70.95; H, 9.11; N, 12.68.

### 5.3. *trans* 2-[2-(5-Bromofuran-2-yl)vinyl]-1,3-dimethylimidazolium iodide (3)

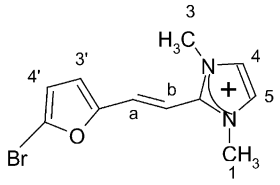


From 5-bromo furan aldehyde (58 mg, 0.334 mmol) and 1,2,3 trimethylimidazolium iodide (80 mg, 0.334 mmol), 2 mL ethanol, 4 drops NaOH. The solution was stirred, 10 min and then the heating was stopped. Yellow prisms. Yield: 32 mg (24.2%); mp 246–247 °C (lit. no mp and NMR available).; MS: $M^+Br_{79}$ 267.1, $M^+Br_{81}$ 269.1; $^1$HNMR (DMSO-$d_6$, δ): 7.37 (d, 1H, $J$ = 16.5 Hz, Ha), 6.87 (d, 1H, $J$ = 16.5 Hz, Hb), 7.72 (s, 2H, H4, H5), 3.31 (s, 6H, H1, H3), 6.99 (d, 1H, $J$ = 3.5 Hz, H3′), 6.83 (d, 1H, $J$ = 3.5 Hz, H4′). Anal. calcd for $C_{12}H_{16}BrIN_2O$: C, 50.54; H, 6.01; N, 9.82. Found: C, 50.47; H, 6.03; N, 9.87.

### 5.4. *trans* 2-[2-[5-(2-Chlorophenyl)furan-2-yl]vinyl]-1,3-dimethylimidazolium iodide (5)

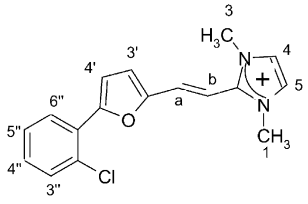


From 5-(2-chlorophenil)furan aldehyde (0.1 g, 0.234 mmol) and 1,2,3 trimethylimidazolium iodide (0.115 g, 0.481 mmol), 2 mL ethanol, 1 drop NaOH. The solution was refluxed for 1 h. Yellow needles. Yield: 118 mg (57%); mp 283 °C dec.; MS: $M^+Cl_{35}$ 298.7, $M^+Cl_{37}$ 300.7; $^1$HNMR (DMSO-$d_6$, δ): 7.51 (d, 1H, $J$ = 17 Hz, Ha), 7.08 (d, 1H, $J$ = 17 Hz, Hb), 3.95 (s, 6H, H1, H3), 7.75 (s, 2H, H4, H5), 7.14 (d, 1H, $J$ = 3.5 Hz, H3′), 7.35 (d, 1H, $J$ = 3.5 Hz, H4′), 7.43 (m, 1H, $J$ = 7.75 Hz; H3″), 7.62 (dd, 1H, $J$ = 7.75 Hz, H2″), 8.10 (dd, 1H, $J$ = 8.25 Hz, H5″), 7.51 (m, 1H, $J$ = 8 Hz, H4″). Anal. calcd for $C_{17}H_{17}ClIN_2O$: C, 67.88; H, 5.70; N, 9.31. Found: C, 67.84; H, 5.72; N, 9.33.

### 5.5. *trans* 2-[2-[5-(4-Bromophenyl)furan-2-yl]vinyl]-1,3-dimethylimidazolium iodide (6)

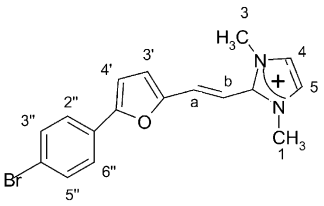

From 5-(4-bromophenil)furan aldehyde (84 mg, 0.177 mmol) and 1,2,3 trimethylimidazolium iodide (80 mg, 0.334 mmol) in 2 mL ethanol with 3 drops of NaOH. Yellow prisms. Yield: 113.6 mg (72%); mp 283–285 °C; MS: $M^+Br_{79}$ 343, $M^+Br_{81}$ 345; $^1$HNMR (DMSO-$d_6$, δ): 6.53 (d, 1H, $J=16.5$ Hz, Ha), 6.12 (d, 1H, $J=16.5$ Hz, Hb), 2.99 (s, 6H, H1, H3), 6.80 (s, 2H, H4, H5), 6.32 (d, 1H, $J=3.5$ Hz, H3′), 6.13 (d, 1H, $J=3.5$ Hz, H4′), 6.92 (d, 2H, $J=8.5$ Hz, H3″, H5″), 7.62 (d, 2H, $J=8.5$ Hz, H2″, H6″). Anal. calcd for $C_{18}H_{20}BrIN_2O$: C, 59.84; H, 5.86; N, 7.75;. Found: C, 59.89; H, 5.83; N, 7.73.

### 5.6. *cis* 2-[2-(Thiophen-2-yl)vinyl]-1, 3-dimethylimidazolium iodide (7)

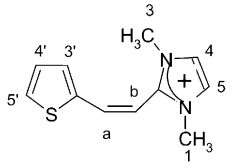

From 2-thiophencarboxaldehyde (41.66 μL, 0.45 mmol) and 1,2,3 trimethylimidazolium iodide (106.1 mg, 0.45 mmol), 2 mL ethanol, 71.33 μL NaOH. White needles. Yield: 83 mg (56.1%); mp 285–288 °C; MS: $M^+$ 205; $^1$H NMR (DMSO-$d_6$, δ): 7.69 (d, 1H, $J=12$ Hz, Ha), 6.30 (d, 1H, $J=11.5$ Hz, Hb), 3.63 (s, 6H, H1, H3), 7.90 (s, 2H, H4, H5), 7.32 (d, 1H, $J=3$ Hz, H3′), 7.14 (dd, 1H, $J=5$ Hz, H4′), 7.71 (d, 1H, $J=7$ Hz, H5′). The *cis* configuration was confirmed by a NOE experiment involving irradiation of the Hb ethylenic proton. Anal. calcd for $C_{11}H_{14}IN_2S$: C, 64.04; H, 6.84; N, 13.58; S, 15.54. Found: C, 64.00; H, 6.82; N, 13.61; S, 15.57.

### 5.7. *trans* 2-[2-(5-Bromo-thiophen-2-yl)vinyl]-1,3-dimethylimidazolium iodide (8)

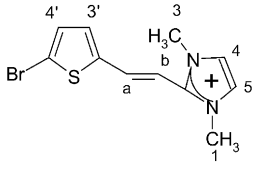

From 5-bromo-2-thiophencarboxaldehyde (39.78 μL, 0.334 mmol) and 1,2,3 trimethylimidazolium iodide (80 mg, 0.334 mmol), 2 mL ethanol, 2 drops NaOH. Yellow prisms. Yield: 52 mg (37%); mp 293 °C dec.; MS: $M^+$ 285; $^1$H NMR (DMSO-$d_6$, δ): 7.67 (d, 1H, $J=16.5$ Hz, Ha), 6.92 (d, 1H, $J=16.5$ Hz, Hb), 7.72 (s, 2H, H4, H5), 3.89 (s, 6H, H1, H3), 7.42 (d, 1H, $J=3.5$ Hz, H4′), 7.34 (d, 1H, $J=3.5$ Hz, H5′). Anal. calcd for $C_{11}H_{13}BrIN_2S$: C, 46.33; H, 4.59; N, 9.82; S, 11.24. Found: C, 46.30; H, 4.57; N, 9.85; S, 11.26.

### 5.8. *trans* 2-[2-(*N*-Metilpyrrol-2-yl)vinyl]-1,3-dimethylimidazolium iodide (9)

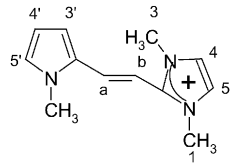

From *N*-methylpyrrol-2-carboxaldehyde (35.9 μL, 0.334 mmol) and 1,2,3 trimethylimidazolium iodide (80 mg, 0.334 mmol), 2 mL ethanol, 67 μL NaOH. The solution was stirred for 7 h. Yellow prisms. Yield: 12 mg (11%); mp 289–291 °C; MS: $M^+$ 203; $^1$H NMR (DMSO-$d_6$, δ): 7.38 (d, 1H, $J=16.5$ Hz, Ha), 6.80 (d, 1H, $J=16.5$ Hz, Hb), 7.68 (s, 2H, H4, H5), 3.90 (s, 6H, H1, H3), 7.03 (m, 1H, H3′), 6.91 (m, 1H, H4′), 6.17 (m, 1H, H5′), 3.74 (s, 3H, H1′). Anal. calcd for $C_{12}H_{17}IN_3$: C, 70.90; H, 8.43; N, 20.67. Found: C, 70.93; H, 8.44; N, 20.69.

### 5.9. *trans* 2-[2-(Thiazol-2-yl)vinyl]-1, 3-dimethylimidazolium iodide (10)

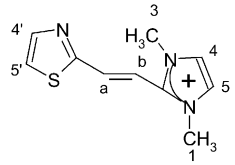

From thiazol-2-carboxaldehyde (39.5 μL, 0.334 mmol) and 1,2,3-trimethylimidazolium iodide (80 mg, 0.334 mmol), 2 mL ethanol, 4 drops NaOH. Yellow prisms. Yield: 22.9 mg (20.5%); mp 278–280 °C; MS: $M^+$ 207; $^1$H MR (DMSO-$d_6$, δ): 7.82 (d, 1H, $J=16.5$ Hz, Ha), 7.46 (d, 1H, $J=16.5$ Hz, Hb), 7.80 (s, 2H, H4, H5), 3.95 (s, 6H, H1, H3), 8.06 (d, 1H, $J=3$ Hz, H4′), 8.08 (d, 1H, $J=3$ Hz, H5′). Anal. calcd for $C_{10}H_{13}IN_3S$: C, 57.94; H, 6.32; N, 20.27; S, 15.47. Found: C, 57.89; H, 6.33; N, 20.28; S, 15.50.

## 6. Biological essays

### 6.1. Human cell lines (LNCap and MCF7)

Human prostate adenocarcinoma cells (LNCap) were grown in RPMI 1640. Human mammary adenocarcinoma (MCF7) were grown in Dulbecco's MEM

(DMEM), 1.0 g/l D-glucose. Each medium was supplemented with 10% (vol/vol) heat-inactivated fetal bovine serum, 2 mM L-Alanyl-L-Glutamine, penicillin-streptomycin (50 units–50 μg for mL) and incubated at 37 °C in humidified atmosphere of 5% $CO_2$, 95% air. The culture medium was changed twice a week.

### 6.2. Treatment with antitumor agents and MTT colorimetric assay

Each human cancer cell line (5×103 cells/0.33 $cm^2$) were plated in 96 well plates 'Nunclon TM Microwell TM' (Nunc) and were incubated at 37 °C. After 24 h, cells were treated with compounds **1**, **2**, **3**, **5**, **6**, **8**, **9** and **11** (final concentration 0.01–100 μM). Untreated cells were used as controls. Microplates were incubated at 37 °C in humidified atmosphere of 5% $CO_2$, 95% air for 3 days and then cytotoxicity was measured with colorimetric assay based on the use of tetrazolium salt MTT (3-(4,5-dimethylthiazol-2-yl)-2,5-diphenyl tetrazolium bromide).[11] The results were read on a multiwell scanning spectrophotometer (Multiscan reader), using a wavelength of 570 nm. Each value was the average of 8 wells (standard deviations were less than 20%). The $GI_{50}$ value was calculated according to NCI: thus, $GI_{50}$ is the concentration of test compound where $100\times(T-T0)/(C-T0) = 50$ (T is the optical density of the test well after a 48-h period of exposure to test drug; T0 is the optical density at time zero; C is the control optical density).

## Acknowledgements

We thank Prof. G. Cruciani (University of Perugia) for helpful discussions. Financial support of the University of Catania and of MIUR (Rome) is also gratefully acknowledged.

## References and notes

1. Ballistreri, A.; Gregoli, L.; Musumarra, G.; Spalletti, A. *Tetrahedron* **1998**, *54*, 9721.
2. Fichera, M.; Fortuna, C. G.; Impallomeni, G.; Musumarra, G. *Eur. J. Org. Chem.* **2002**, 145.
3. Barresi, V.; Condorelli, D. F.; Fortuna, C. G.; Musumarra, G.; Scirè, S. *Bioorg. Med. Chem.* **2002**, *10*, 2899.
4. Ballistreri, F. P.; Barresi, V.; Consiglio, G.; Fortuna, C. G.; Longo, M. L.; Musumarra, G. *Arkivoc* **2003,** *part (i),* 105–117 or at http://www.arkat-usa.org/ark/journal/2003/General/Part(i)_index.htm.
5. Pastor, M.; Cruciani, G.; McLay, I.; Pickett, S.; Clementi, S. *J. Med. Chem.* **2000**, *43*, 3233.
6. GRID v. 20 Molecular Discovery Ltd.
7. Goodford, P. J. *J. Med. Chem.* **1985**, *28*, 849.
8. Boobbyer, D. N. A.; Goodford, P. J.; Mcwhinnie, P. M.; Wade, R. C. *J. Med. Chem.* **1989**, *32*, 1083.
9. Wade, R.; Clerk, K. J.; Goodford, P. J. *J. Med. Chem.* **1993**, *36*, 140.
10. Haugwitz, R. D.; Maurer, B. V.; U.S. Patent 4,006,137, 1977; *Chem. Abstr.* **1977**, *87,* 5971y.
11. Mosmann, T. J. *J. Immunol. Meth* **1983**, *65*, 55.